

Increasing the spectral efficiency of DDO-CE-OFDM systems by multi-objective optimization

Citation for published version (APA):

de Rocha, H. R. O., Dias, V. O. C., da Veiga Pereira, E., Nunes, R. B., Segatto, M. E. V., & Silva, J. A. L. (2019). Increasing the spectral efficiency of DDO-CE-OFDM systems by multi-objective optimization. *Journal of Lightwave Technology*, 37(9), 2155-2162. [8640082]. <https://doi.org/10.1109/JLT.2019.2898945>

Document license:
TAVERNE

DOI:
[10.1109/JLT.2019.2898945](https://doi.org/10.1109/JLT.2019.2898945)

Document status and date:
Published: 01/05/2019

Document Version:
Publisher's PDF, also known as Version of Record (includes final page, issue and volume numbers)

Please check the document version of this publication:

- A submitted manuscript is the version of the article upon submission and before peer-review. There can be important differences between the submitted version and the official published version of record. People interested in the research are advised to contact the author for the final version of the publication, or visit the DOI to the publisher's website.
- The final author version and the galley proof are versions of the publication after peer review.
- The final published version features the final layout of the paper including the volume, issue and page numbers.

[Link to publication](#)

General rights

Copyright and moral rights for the publications made accessible in the public portal are retained by the authors and/or other copyright owners and it is a condition of accessing publications that users recognise and abide by the legal requirements associated with these rights.

- Users may download and print one copy of any publication from the public portal for the purpose of private study or research.
- You may not further distribute the material or use it for any profit-making activity or commercial gain
- You may freely distribute the URL identifying the publication in the public portal.

If the publication is distributed under the terms of Article 25fa of the Dutch Copyright Act, indicated by the "Taverne" license above, please follow below link for the End User Agreement:

www.tue.nl/taverne





Take down policy

If you believe that this document breaches copyright please contact us at:

openaccess@tue.nl

providing details and we will investigate your claim.

Increasing the Spectral Efficiency of DDO-CE-OFDM Systems by Multi-Objective Optimization

Helder Roberto de O. Rocha, Vinicius O. C. Dias, Esequiel da Veiga Pereira , Reginaldo Barbosa Nunes , Marcelo E. V. Segatto , *Member, IEEE, Member, OSA*, and Jair A. L. Silva , *Member, IEEE*

Abstract—A multi-objective optimization was implemented to increase the spectral efficiency of direct-detection optical orthogonal frequency division multiplexing (OFDM) systems with constant-envelope (CE) signals. Based on a genetic algorithm, the optimization procedure evaluates the impact of fiber injection power in the reduction of the guard band between the optical carrier and the CE-OFDM signals, optimizing important parameters such as electrical phase modulation and optical modulation indices of the denominated DDO-CE-OFDM system. Simulation results show that a guard-band reduction around 40% was achieved in a 4 Gbps optimized DDO-CE-OFDM system with 16-QAM subcarrier mapping and -7 dBm fiber input power. Results obtained in an experimental proof-of-concept conducted to validate the optimization procedure show that this reduction can reach 66% according to a power penalty of ≈ 2 dB demanded by the inherent spectral broadening of CE-OFDM signals, after propagation over 40 km of standard single-mode fiber.

Index Terms—Constant-envelope optical OFDM, multi-objective optimization, NSGA II, spectral efficiency.

I. INTRODUCTION

PROPOSED by S. C. Thompson *et al.* in Ref. [1] to increase the power Amplification efficiency in wireless systems, the constant envelope orthogonal frequency division multiplexing (CE-OFDM) approach is basically a peak-to-average power ratio (PAPR) reduction technique. Based on electrical phase

Manuscript received September 20, 2018; revised December 10, 2018 and January 16, 2019; accepted February 8, 2019. Date of publication February 12, 2019; date of current version April 11, 2019. This work was supported in part by PRONEX/FAPES-280/2018, in part by FAPES-538/2018, in part by FAPES-601/2018, in part by CNPq-307757/2016-1, in part by CNPq-304564/2016-8, in part by CNPq-309823/2018-8, and in part by NiDA projects. (*Corresponding author: Jair A. L. Silva.*)

H. R. de O. Rocha, M. E. V. Segatto, and J. A. L. Silva are with the Department of Electrical Engineering, Federal University of Espírito Santo, 29075-910 Vitória-ES, Brazil (e-mail: helder.rocha@ufes.br; segatto@ele.ufes.br; jair.silva@ufes.br).

V. O. C. Dias is with the Signal Processing Systems Group, Department of Electrical Engineering, Eindhoven University of Technology, 5600 MB Eindhoven, The Netherlands (e-mail: vinicius.oliari@gmail.com).

E. da V. Pereira is with the Department of Computer and Electronics, Federal University of Espírito Santo, 29932-540 São Mateus-ES, Brazil (e-mail: esequiel.pereira@ufes.br).

R. B. Nunes is with the Department of Electrical Engineering, Federal Institute of Espírito Santo, 29075-910 Vitória-ES, Brazil (e-mail: regisbn@ifes.edu.br).

Color versions of one or more of the figures in this paper are available online at <http://ieeexplore.ieee.org>.

Digital Object Identifier 10.1109/JLT.2019.2898945

modulation, this transformation method reduces the PAPR of conventional OFDM signals to 0 dB.

Taking advantage of this concept, in [2] we proposed and experimentally demonstrated the transmission of constant envelope (CE) signals in direct detection optical OFDM (DDO-OFDM) systems to increase the tolerance to the intermodulation effects introduced by the Mach-Zehnder modulator (MZM). The adaptation that allowed the transmission of CE-OFDM signals with PAPR = 3 dB was subsequently available to mitigate fiber nonlinearity in the nominated DDO-CE-OFDM system, as described in [3]. Indeed, the simulation results described in [3] and the experimental demonstration presented in [4] show that, evaluating the above-mentioned tolerance, the CE based system outperforms conventional DDO-OFDM systems over dispersion uncompensated standard single-mode fibers (SSMF), despite the spectral efficiency (SE) reduction that characterizes phase modulation schemes [5]. Subcarrier multiplexing can be implemented with the discrete Hartley transform (DHT) proposed in [6] to cope with SE degradation. The authors of the numerical analysis presented in [7] show that performance improvements can be achieved with a combination of DHT multiplexing and the above-mentioned CE modulation.

In this paper, we expand the optimization process outlined in [8] to DDO-CE-OFDM systems in order to address the trade-off imposed by spectral broadening and system performance. The relevance of the phase modulation index h of such systems was also demonstrated in the experimental work described in [9], in which the authors prove the fiber nonlinearity and phase noise tolerance of CE-OFDM signals based on optical phase modulation (OPM) in the W-band (75-110 GHz). The performance of such systems increases with large values of h , thanks to a spectral enlargement that limits the guard band reductions extensively studied in [8].

Transmission over the OPM based long-haul link reported in [10] can be achieved in optical intensity modulation if the dynamic range of MZM modulators is explored by a proper choice of the optical modulation index, as suggested by the optical carrier suppression presented in [11]. Matched to an optimization that deals with the MZM bias point, concomitant performance and spectral efficiency (SE) improvements are feasible.

Therefore, a spectral efficiency enhancement, based on parameter optimization, of DDO-CE-OFDM systems is

highlighted in this work. A problem formulation, solved by an elitist nondominated sorting Genetic algorithm (NSGA), is proposed to minimize the fiber launch power and the guard band required to a system bit-error-rate $\text{BER} \leq 10^{-3}$. Numerical simulation results show that, with a fiber injection power of -7 dBm, a guard-band reduction around 40% was achieved in a 4 Gbps optimized DDO-CE-OFDM system, with 16-QAM sub-carrier mapping. An experimental proof-of-concept validates the robustness of the optimization procedures, according to a 66% guard band reduction obtained by the system after propagation over 40 km of SSMF, with a power penalty of ≈ 2 dB.

The remainder of this paper is organized as follows. A theoretical background of the CE-OFDM signal generation and detection in intensity modulated and direct detection (IMDD) optical systems is presented in Section II. The proposed multi-objective optimization algorithm is presented in Section III. The simulation results obtained with the SE procedures and the experimental validation are discussed in Sections IV and V, respectively. Concluding remarks are provided in Section VI.

II. THEORETICAL BACKGROUND

In this Section we develop the fundamentals of generation and detection of CE-OFDM signals in intensity-modulated and direct-detection (IMDD) optical systems.

A. CE-OFDM Signal Generation

The CE-OFDM signals of this work were generated by phase modulating an electrical carrier with conventional OFDM waveforms. Thereby, the constant-envelope bandpass signals with PAPR = 3 dB can be expressed as

$$c(t) = A \cos[2\pi f_c t + \theta_n + 2\pi h \cdot x(t)], \quad (1)$$

where A is the signal amplitude, f_c is the carrier frequency, θ_n is a phase continuous memory term, h is the phase modulation index and $x(t) = C \sum_{k=1}^{N_s-1} \Re[X(k)] \cos\left(\frac{2\pi kt}{T}\right) - \Im[X(k)] \sin\left(\frac{2\pi kt}{T}\right)$ the OFDM waveforms, with $\{X(k)\}_{k=1}^{N_s-1}$ the M -QAM data symbols, $T = \frac{N}{F_s}$ the signaling interval duration, $N = 2N_s + 2$ the fast-Fourier transform length, F_s the sampling rate and C a constant. The bandwidth of $c(t)$ is usefully expressed as $B = \max(2\pi h, 1)B_W$ Hz, which is a root-mean-square (RMS) bandwidth, lower bounded by the bandwidth (B_W) of $x(t)$ [3].

B. Direct-Detection of CE-OFDM Signals in Optical Systems

The investigated IMDD optical system uses the same single arm Mach-Zehnder modulator described in [8]. Therefore, the optical field at output of the MZM is given by

$$E_{MZM}(t) = \cos\left[\frac{\pi c(t)}{2V_\pi} - \frac{\pi V_{bias}}{2V_\pi}\right] \cdot \sqrt{2P} \cos(w_0 t), \quad (2)$$

where V_π is its switching voltage, P is the power of the continuous wave (CW) laser signal at the MZM optical input and $w_0 = 2\pi f_0$ the optical signal central frequency.

After optical pre-amplification and photodetection, the output current i_{PIN} of the photodiode with responsivity R is

proportional to RE_{PIN}^2 , with

$$\begin{aligned} E_{PIN}^2(t) = & \cos^2\left[\frac{\pi}{2V_\pi}(c(t) - V_{bias})\right] \cdot 2GP \cos^2(2\pi f_0 t) \\ & + n_i^2 \cos^2(2\pi f_0 t) + n_q^2 \sin^2(2\pi f_0 t) \\ & + 2 \cos^2(2\pi f_0 t) n_i(t) \sqrt{2GP} \\ & \times \cos\left[\frac{\pi}{2V_\pi}(c(t) - V_{bias})\right] \\ & + 2n_q^2(t) \sin(2\pi f_0 t) \cos(2\pi f_c t) \\ & \times \left\{ n_i(t) + 2\sqrt{2GP} \cos\left[\frac{\pi}{2V_\pi}(c(t) - V_{bias})\right] \right\}, \end{aligned} \quad (3)$$

for G the amplification gain, $n_i(t)$ and $n_q(t)$ the noise in-phase and quadrature components with power spectral density given by $N_{ASE}/2$ and variance $\sigma_n^2 = N_{ASE} \cdot B_o$, for B_o the bandwidth of the optical filter at its output.

After some simplifications with trigonometric identities¹ and neglecting high frequency contributions ($f > f_0 + B_o/2$),

$$\begin{aligned} i_{PIN}(t) = & R \left[GP \cos^2\left(\frac{\pi}{2V_\pi}(c(t) - V_{bias})\right) \right. \\ & + n_i(t) \sqrt{2GP} \cos\left(\frac{\pi}{2V_\pi}(c(t) - V_{bias})\right) \\ & \left. + \frac{1}{2}(n_i^2(t) + n_q^2(t)) \right] \\ = & \frac{R}{2} \left\{ GP \left[1 + \cos\left(\frac{\pi}{V_\pi}(c(t) - V_{bias})\right) \right] \right. \\ & + 2n_i(t) \sqrt{2GP} \cos\left(\frac{\pi}{2V_\pi}(c(t) - V_{bias})\right) \\ & \left. + n_i^2(t) + n_q^2(t) \right\}. \end{aligned} \quad (4)$$

Considering the first-order Taylor expansion that allows $\cos(Gc(t) + H) \approx \cos(H) - Gc(t) \sin(H)$, the received bandpass signal becomes

$$\begin{aligned} i_{PIN}(t) \approx & \frac{R}{2} \left\{ GP \left[1 + \cos\left(\frac{\pi V_{bias}}{V_\pi}\right) \right. \right. \\ & + \left. \frac{\pi c(t)}{V_\pi} \sin\left(\frac{\pi V_{bias}}{V_\pi}\right) \right] \\ & + 2n_i(t) \sqrt{2GP} \left[\cos\left(\frac{\pi V_{bias}}{2V_\pi}\right) \right. \\ & + \left. \frac{\pi c(t)}{2V_\pi} \sin\left(\frac{\pi V_{bias}}{2V_\pi}\right) \right] \\ & \left. + n_i^2(t) + n_q^2(t) \right\}. \end{aligned} \quad (5)$$

If $n_i^2(t)$ and $n_q^2(t)$ are significantly smaller than the carrier, after filtering the DC-component, the photocurrent can be

¹ $\sin(\theta) \cos(\theta) = \frac{1}{2} \sin(2\theta)$, $\sin^2(\theta) = \frac{1 - \cos(2\theta)}{2}$, $\cos^2(\theta) = \frac{1 + \cos(2\theta)}{2}$

simplified to

$$i_{PIN}(t) \approx K_1 \cos[w_c t + s(t)] + K_2(t)n_i(t), \quad (6)$$

for $w_c = 2\pi f_c$, $s(t) = 2\pi h x(t)$,

$$K_1 = \frac{ARGP\pi \sin\left(\frac{\pi V_{bias}}{V_\pi}\right)}{2V_\pi}, \quad (7)$$

and

$$K_2(t) = R\sqrt{2GP} \left[\cos\left(\frac{\pi V_{bias}}{2V_\pi}\right) + \frac{\pi c(t)}{2V_\pi} \sin\left(\frac{\pi V_{bias}}{2V_\pi}\right) \right]. \quad (8)$$

Finally, if we apply a downconversion at the signal of eq. (6), with complex signals generated by the definition $\mathbb{H}_M : \mathbb{R} \rightarrow \mathbb{C}$, $\mathbb{H}_M : g(t) \rightarrow [g(t), \mathbb{H}\{g(t)\}]$, for $\mathbb{H}\{\cdot\}$ the Hilbert transform, the baseband CE-OFDM signal can be recovered as follows

$$\begin{aligned} \mathbb{H}_M\{i_{PIN}(t)\}e^{-jw_c t} &\approx K_1 \cos[w_c t + s(t)]e^{-jw_c t} \\ &\quad + K_2(t)n_i e^{-jw_c t} \\ &\quad + j\{K_1 \sin[w_c t + s(t)]e^{-jw_c t}\} \\ &\quad + \mathbb{H}\{K_2(t)n_i\}e^{-jw_c t} \\ &= K_1 \frac{e^{js(t)} + e^{-j[2w_c t + s(t)]}}{2} \\ &\quad + K_2(t)n_i e^{-jw_c t} + \\ &\quad + j(K_1 \frac{e^{js(t)} - e^{-j[2w_c t + s(t)]}}{2j}) \\ &\quad + \mathbb{H}\{K_2(t)n_i\}e^{-jw_c t} \\ &= K_1 e^{js(t)} + K_2(t)n_i e^{-jw_c t} \\ &\quad + j\mathbb{H}\{K_2(t)n_i\}e^{-jw_c t} \\ &= K_1 \cos(s(t)) + K_2(t)n_i \cos(w_c t) \\ &\quad + \mathbb{H}\{K_2(t)n_i\} \sin(w_c t) + \\ &\quad + j[K_1 \sin[s(t)] - K_2(t)n_i \sin(w_c t)] \\ &\quad + \mathbb{H}\{K_2(t)n_i\} \cos(w_c t). \end{aligned} \quad (9)$$

The inverse operations to those performed at the electrical transmitter are performed at the receiver. A discrete phase demodulator is implemented by an arc-tangent processor that simply calculates its argument, followed by a phase unwrapper in order to minimize the effect of phase ambiguities. From eq. (9), the CE-OFDM signal is derived as

$$\hat{s}(t) = \arctan \left(\frac{\mathbb{H}\{\mathbb{H}_M\{i_{PIN}(t)\}e^{-jw_c t}\}}{\mathbb{R}\{\mathbb{H}_M\{i_{PIN}(t)\}e^{-jw_c t}\}} \right), \quad (10)$$

or equivalently by

$$\begin{aligned} \hat{s}(t) = \arctan \left\{ \frac{K_1 \sin[2\pi h x(t)] - K_2(t)n_i \sin(w_c t) + \dots}{K_1 \cos[2\pi h x(t)] + K_2(t)n_i \cos(w_c t) + \dots} \right. \\ \left. \dots \frac{+\mathbb{H}\{K_2(t)n_i\} \cos(w_c t)}{+\mathbb{H}\{K_2(t)n_i\} \sin(w_c t)} \right\}. \end{aligned} \quad (11)$$

TABLE I
PROBLEM FORMULATION

Min. P_{out} @ BER $\leq 10^{-3}$
Min. $\left(\frac{B_G}{B_w}\right)$
s.t.
$0.013 \times V_\pi \leq OMI \leq 0.08 \times V_\pi$
$0.1 \leq h \leq 0.9$
$0.1 \times B_w \leq B_G \leq B_w$
$0.5 \times V_\pi \leq V_{bias} < 1.36 \times V_\pi$
$(2^{X_{max}})^{-1} \leq GI = (2^X)^{-1} \leq (2^{X_{min}})^{-1}$
$V_\pi = 4.4V$
$X_{min} = 2$
$X_{max} = 10$

It can be observed from eq. (11) that, in the absence of noise, $\hat{s}(t) = 2\pi h \cdot x(t)$.

III. THE MULTI-OBJECTIVE OPTIMIZATION PROCEDURE

In the multi-objective optimization procedure, a problem formulation was proposed to minimize both fiber launch power (P_{out}) and guard band required to a system BER $\leq 10^{-3}$, subject to the constraints shown in Table I.

It can be verified from equations (1) and (2) that, the optical modulation index defined as $OMI = (C_{in})_{RMS}/V_\pi$, with $(C_{in})_{RMS}$ the RMS amplitude of $c(t)$, plays an important role in the formulated problem. Large and extremely low values of the CE-OFDM signal amplitude (A) should be avoided due to the MZM induced nonlinearity and performance degradation, respectively [2].

The index h is another crucial parameter in the formulation because of the already mentioned tradeoff between spectral broadening and performance [3]. Low values of the phase modulation index leads to noise vulnerabilities of the DDO-CE-OFDM system. On the other hand, the system performance improves with higher values of h , at the expense of a bandwidth enlargement that decreases the SE. Hence, beyond the SE penalties provided by the intermodulation distortions (IMD) described in [12], the spectral broadening generated by CE-OFDM signals with large values of h limits a desired guard band (B_G) reduction.

It is well known that the MZM should be biased in the range $V_\pi/2 \leq V_{bias} < V_\pi$, in order to address the tradeoff between the MZM nonlinearity and receiver sensitivity [8]. A limit above V_π was established in the formulation in order to explore the constant envelope characteristics of employed electrical signals. The cyclic prefix also recommended in CE-OFDM based systems to combat inter-symbol interference is optimized, considering base-2 exponents between $X_{min} = 2$ and $X_{max} = 10$, bearing in mind the introduced overhead.

To solve the problem formulated in Table I, we used an Elitist Nondominated Sorting Genetic Algorithm (NSGA-II), an elitist evolutionary algorithm that preserves dominant solutions through the generations [13]. The optimization begins with a randomly ordered population of P solutions. Tournament selection, crossover and mutation are the Genetic operators applied to create the next generation Q , with fitness values that define the dominance in the population. Thereafter, a single population

TABLE II
OFDM PARAMETERS

Parameter	Value
Effective bandwidth B_w	1 GHz
FFT size N	1024
Data subcarriers N_s	512
Subcarrier mapping M	16-QAM [4-QAM]
Nominal bit rate $R_b = B_w \times \log_2(M)$	4 Gbps [2 Gbps]

$R = P \cup Q$ is obtained, in which N solutions are selected to produce a new P population. This process is repeated during a pre-defined number of generations. Populations of 20 solutions for OMI , h , B_G , V_{bias} and GI were randomly generated in the beginning of the proposed procedure. Then, tournament selection at a rate of 0.95, Blend crossover (Blx- α) with $\alpha = 0.4$ and mutation at a rate of 0.05 are implemented to provide an efficient algorithm evolution [14].

IV. INCREASING THE SYSTEM SPECTRAL EFFICIENCY THROUGH THE OPTIMIZATION PROCEDURE

To evaluate the robustness of the formulated problem, we conduct Monte Carlo simulations of a numerical model of the DDO-CE-OFDM system shown in Fig. 4, for one of the NSGA-II solutions. The performance of the optimized systems was evaluated with the error vector magnitude (EVM) metric described in [15]. Modeled as an additive white Gaussian noise (AWGN), the amplified spontaneous emission (ASE) noise is dominant in the channel model. Table II shows the OFDM parameters used in the simulations. The uncompensated standard single-mode fibers (SSMF) employed in the optical links considers a loss of $\alpha = 0.2$ dB/km, a dispersion of $D = 17$ ps/(nm.km) and an effective area $A_{eff} = 8 \times 10^{-11}$.

Obtained by the optimization procedures, the Pareto fronts depicted in Figs. 1.(a) and 1.(b) show the MZM output power, i.e., the fiber launch power, against guard band reductions represented by different values of $\frac{B_G}{B_w}$, in back-to-back (B2B) configuration and after propagation through 40 km of uncompensated SSMF. It should be noticed that, the achieved optical powers at a determined $\frac{B_G}{B_w}$ assures the intended $BER \leq 10^{-3}$.

Fig. 1.(a) shows that, a guard band of approximately 30% of the signal useful bandwidth can be achieved with the same MZM output power ($P_{out} = -18$ dBm) required at $B_G = B_w$, for 4-QAM mapping. Low values of B_G can be achieved according to increases in P_{out} , as 14.7 dB more power is required to reach a $\frac{B_G}{B_w}$ of $\approx 14.1\%$. The optimization algorithm provided a minimum guard band of 31.7% at $P_{out} = -3.3$ dBm, when 16-QAM is used as subcarrier mapping. The same behaviour occurred after propagation through the 40 km of SSMF, despite the expected higher values of the demanded fiber injection powers. Fig. 1.(b) shows that, for 4-QAM subcarrier mapping, a $B_G = 0.319 \times B_w$ is obtained with a $P_{out} = -10.5$ dBm, whereas an optical power of 3.5 dBm is required at a guard band of only 17.5% of the signal bandwidth. For 16-QAM, a minimum guard band of 343 MHz is needed without significant power penalties. Tables III and IV show details of the main optimized parameters obtained in both considered scenarios.

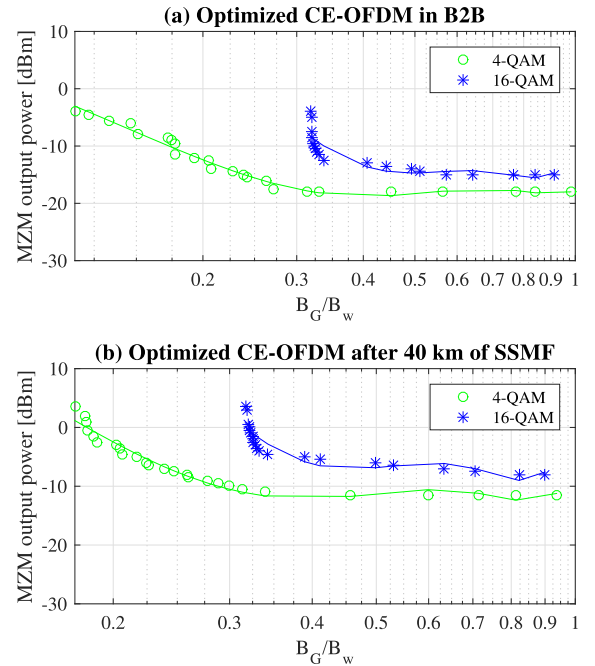


Fig. 1. MZM output power versus $\frac{B_G}{B_w}$ of optimized DDO-CE-OFDM systems in (a) B2B and (b) after 40 km of SSMF.

In order to emphasize the robustness of the optimization processes, we also conducted simulations of the optimized DDO-CE-OFDM systems in an optical link with 40 km of SSMF, varying some optimized parameters. Fig. 2 shows that performance degradation occurs through deviations in the optimized values of optical modulation index and MZM polarization point. It is clear from the surface plotted in Fig. 2 that the best EVM performance ($EVM = -9.84$ dB) is guaranteed with the parameters showed in the fifth line of Table IV, when 4-QAM is the subcarrier modulation.

In the surface depicted in Fig. 3 the performance penalties are registered due to deviations in the optimized values of phase modulation index and $\frac{B_G}{B_w}$. Here also, it is clear that, for 16-QAM mapping, the best performance ($EVM = -15.66$ dB) is guaranteed by the parameters showed in the last line of Table IV.

Moreover, it should be stressed that, the optimization procedure should be executed whenever the length of the fiber link is changed. Indeed, different amounts of fiber launch power are expected for different fiber lengths, as suggested by the Pareto fronts depicted in Fig. 1.

V. EXPERIMENTAL VALIDATION OF THE OPTIMIZATION PROCEDURES

In this section, we discuss the experimental results to validate the optimization procedures, mainly focused on spectral efficiency attributed to the guard band reductions.

A. Experimental Setup

A block diagram of the setup used to substantiate the SE provided by the optimization is illustrated in Fig. 4. Pseudorandom binary sequences $PRBS = \log_2(M) \times (2^9)$ were mapped

TABLE III
OPTIMIZED PARAMETERS FOR THE PARETO FRONT IN B2B. BER_s : SIMULATED; BER_m : MEASURED

QAM	Optimized Parameters					Objective functions		Simulated		Measured	
M	OMI	V_{bias}	B_G (MHz)	GI	h	P_{out} (dBm)	B_G/B_W	EVM_s	BER_s	EVM_m	BER_m
4	0.10	3.88	141	1/256	0.33	-3.3	0.141	-9.80	0.0010	-9.7138	0.0006
4	0.15	3.77	177	1/256	0.41	-9.5	0.177	-9.47	0.0010	-9.2139	0.0011
4	0.33	3.88	294	1/512	0.59	-18.0	0.294	-9.56	0.0009	-8.6693	0.0026
16	0.07	3.80	317	1/64	0.27	-3.3	0.317	-16.51	0.0010	-14.5606	0.0022
16	0.28	3.90	421	1/64	0.47	-13.5	0.421	-15.55	0.0009	-15.4493	0.0011
16	0.29	3.96	618	1/64	0.49	-15.0	0.618	-15.50	0.0008	-14.3120	0.0018

TABLE IV
OPTIMIZED PARAMETERS FOR THE PARETO FRONT AFTER 40 KM OF SSMF. EVM_s : SIMULATED; EVM_m : MEASURED

QAM	Optimized Parameters					Objective functions		Simulated		Measured	
M	OMI	V_{bias}	B_G (MHz)	GI	h	P_{out} (dBm)	B_G/B_W	EVM_s	BER_s	EVM_m	BER_m
4	0.14	3.76	175	1/8	0.44	3.5	0.175	-8.95	0.0010	-9.5460	0.0011
4	0.18	3.83	197	1/32	0.43	-4.5	0.197	-9.46	0.0008	-9.9378	0.0007
4	0.34	3.90	319	1/128	0.56	-10.5	0.319	-9.84	0.0007	-8.7237	0.0023
16	0.09	3.81	319	1/64	0.36	3.5	0.319	-16.62	0.0010	-14.5014	0.0020
16	0.23	3.81	343	1/128	0.38	-5.0	0.343	-15.52	0.0009	-14.6853	0.0019
16	0.32	3.91	634	1/4	0.47	-7.0	0.634	-15.66	0.0008	-14.7600	0.0016

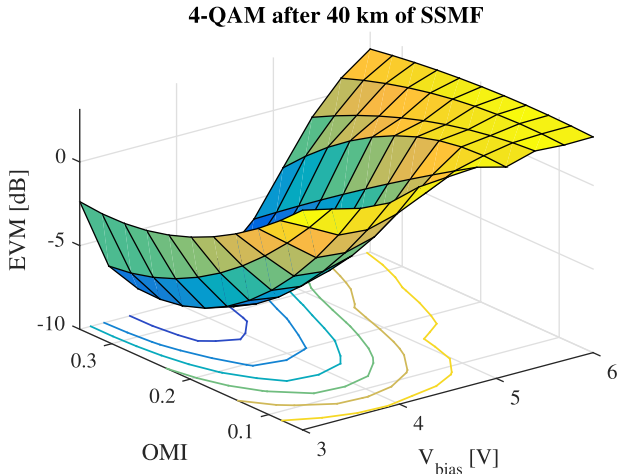


Fig. 2. EVM against optimized values of OMI and V_{bias} .

in 4-QAM ($M = 4$) and 16-QAM ($M = 16$) before frequency multiplexing of 512 data subcarriers by an inverse fast-Fourier transform (IFFT) size of 1024. At the upconversion composed by oversampling, windowing and filtering, the OFDM signals modulates the phase of an electrical carrier centered at f_c , as described in the Refs. [3] and [4]. The importance of the phase modulation index denoted by the parameter $2\pi h$ will be reported in the experimental results.

The 300 CE-OFDM signals with PAPR = 3 dB (see inset 2 of Fig. 4), performed offline using MATLAB, are loaded to the 24 Gsamples/s AWG7122 arbitrary waveform generator, before analog low-pass filtering by a 3 GHz amplifier. Employing a conventional MZM, the bandpass signals modulate the laser source centered at $\lambda = 1550$ nm.

An erbium doped fiber amplifier (EDFA) and an optical filter are used to compensate the MZM insertion loss and to reduce the consequent amplified spontaneous emission noise, respectively. The fiber injection power is tuned by an attenuator

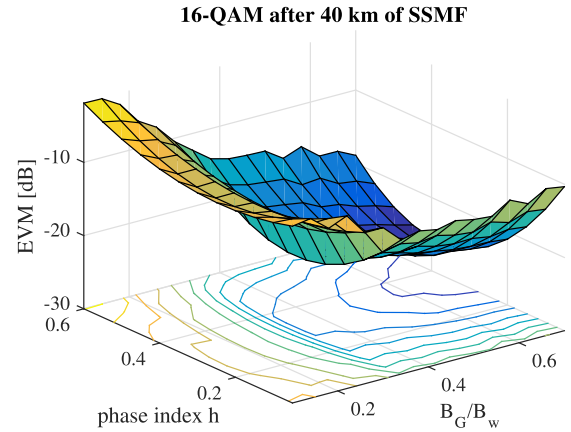


Fig. 3. EVM against optimized values of h and $\frac{B_G}{B_w}$.

embedded in the CW laser driver. A photodiode is used to detect the double-side band signals (see inset 1 of Fig. 4) in B2B and after propagation through 40 km of SSMF. After a sampling process by the 100 Gsamples/s oscilloscope and a time domain synchronization, the recorded photocurrents were processed offline. A discrete phase demodulation, provided by an arctangent signal processing and a phase unwrapping, is implemented before demultiplexing of OFDM signals impaired by linear channel distortions [3], [4]. The arctangent extracts the phase of the CE-OFDM baseband signals through the argument obtained from the demodulator input samples. The phase unwrapping minimizes the effect of phase ambiguities adding multiples of $\pm 2\pi$ when a jump greater than π occurs between consecutive samples of the message signals [1].

B. The Robustness of the Phase Index Optimization

Because of its importance in CE-OFDM signal formats, it is crucial to evaluate the effect of the phase modulation index h in the concerned optimized optical systems. Hence, using the

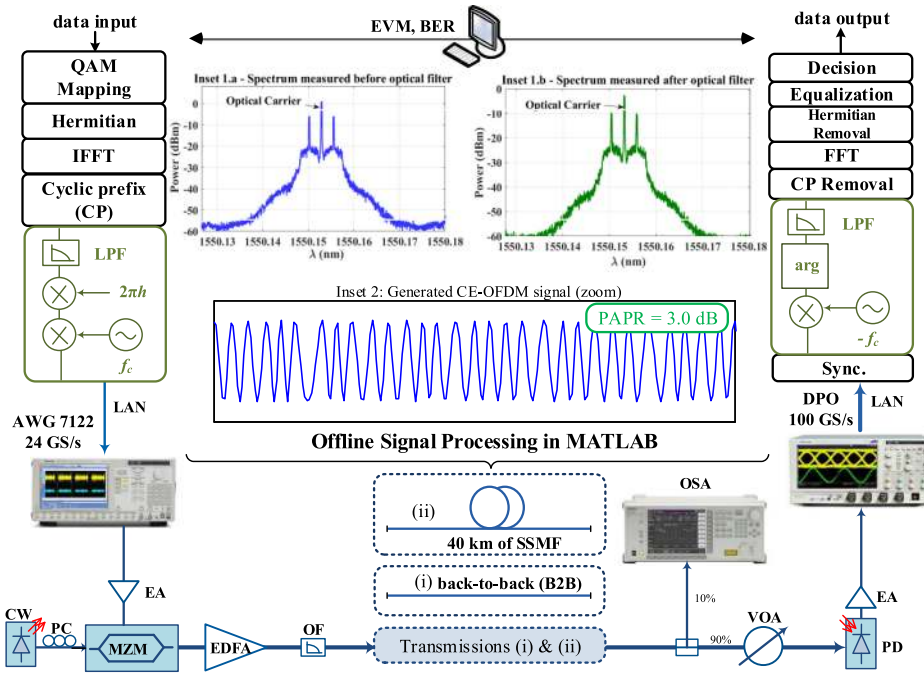


Fig. 4. Experimental setup of the DDO-CE-OFDM system. QAM: Quadrature Amplitude Modulation; (I)FFT: (inverse) fast Fourier transform; CP: Cyclic Prefix; LPF: Low-Pass Filter; EA: Electrical Amplification; CW: Continuous Wave; PC: Polarization Controller; MZM: Mach-Zehnder Modulator; OF: Optical Filter; VOA: Variable Optical Attenuator; PD: Photodetector; Sync: synchronism.

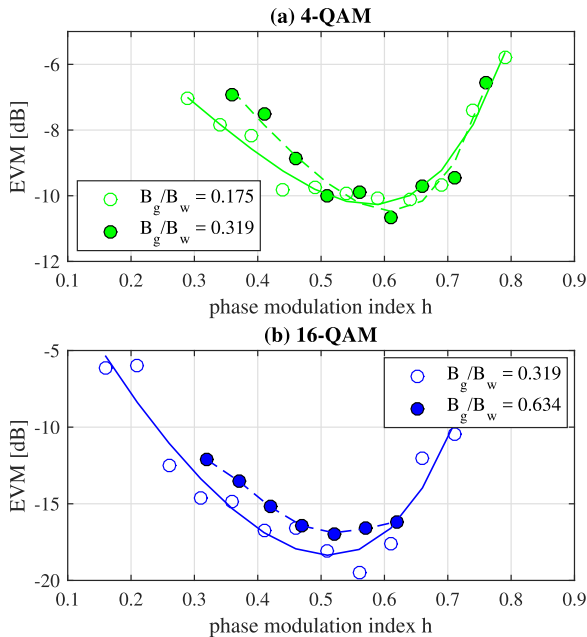


Fig. 5. EVM as a function of different phase modulation index h for (a) 4-QAM and (b) 16-QAM subcarrier mappings.

optimized parameters shown in Table IV, Figs. 5.(a) and 5.(b) show the EVM against index h of the optimized DDO-CE-OFDM systems after propagation through 40 km of SSMF, for 4 and 16-QAM subcarrier mappings, respectively.

As expected, the regions limited by noise and by the modulation nonlinearity are easily identified. Nevertheless, for all considered guard bands, optimal regions can be defined in the

phase index ranges $0.44 \leq h < 0.7$ and $0.35 \leq h < 0.6$ for 4 and 16-QAM, respectively. It is straightforwardly noticed from the optimized parameters of Table IV that, the optimized phase modulation index belongs to the mentioned optimal region. They do not correspond to the quantities that provide the lowest EVM values due to the performance versus spectral efficiency trade-off, mitigated by the proposed multi-objective optimization procedure.

C. Mitigating the Trade-off Between Performance and Spectral Efficiency Through the Proposed Optimization

Fig. 6 show EVM performance evaluations according to variations in the fiber launch power (P_L), after propagation through 40 km of SSMF. Some measured values of $BER \neq 0$ are depicted insight Fig. 6 for performance comparison. Fig. 6.(a) and Table IV show that, for 4-QAM subcarrier mapping, the DDO-CE-OFDM system must add ≈ 14 dB in the injection power to halve B_G/B_W , decreasing the guard band from 31.9 to 17.5%, as advanced by the optimization results provided in Fig. 1. To halve guard band at 16-QAM mapping (see 6.(b)), the demanded launch power is around 10.5 dB. The proximity between the measured (EVM_m and BER_m) and the simulated (EVM_s and BER_s) performance values should be emphasized, as illustrated by the results presented in Table IV and in Fig. 6.

A comparison with the 1% guard band stated in Ref. [8] for direct-detection of optical OFDM signals after propagation through 40 km of SSMF, raised at this point. Indeed, without substantial power penalties (see Fig. 1), the maximum guard band reductions obtained in the investigated DDO-CE-OFDM systems are $\approx 32\%$ and $\approx 34\%$ for 4-QAM and 16-QAM

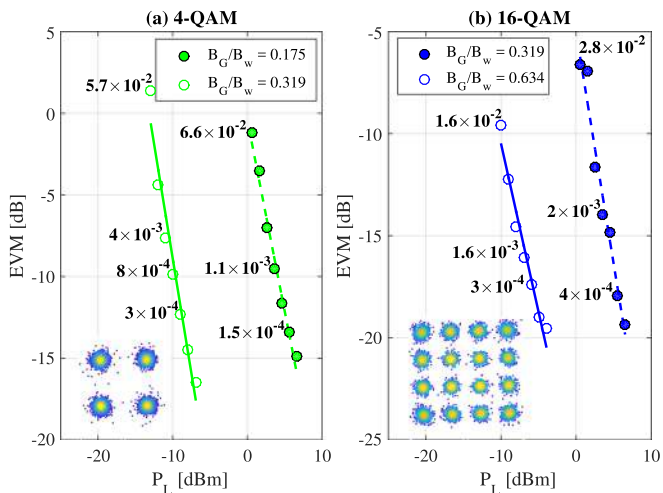


Fig. 6. EVM versus fiber launch power for (a) 17.5% ($\text{OMI} = 0.14$) and 31.9% ($\text{OMI} = 0.34$) of guard band after 40 km of SSMF and 4-QAM mapping, and (b) 31.9% ($\text{OMI} = 0.09$) and 63.4% ($\text{OMI} = 0.32$) of guard band after 40 km of SSMF and 16-QAM mapping. The constellations shown inset were measured for $P_L = -8$ dBm and $P_L = -4$ dBm at the lowest SE of each mapping.

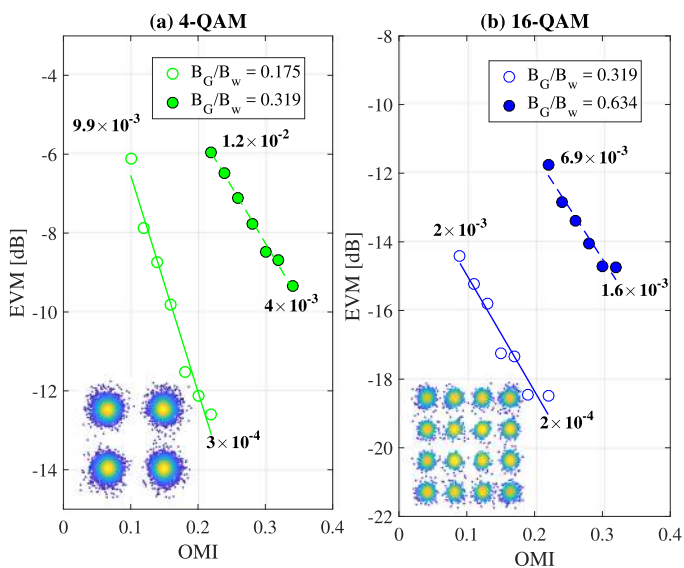


Fig. 7. EVM versus OMI for (a) 17.5% ($P_{\text{out}} = 3.5$ dBm as showed in Table IV) and 31.9% ($P_{\text{out}} = -10.5$ dBm as showed in Table IV) of guard band after 40 km of SSMF and 4-QAM, and (b) 31.9% ($P_{\text{out}} = 3.5$ dBm as showed in Table IV) and 63.4% ($P_{\text{out}} = -7.0$ dBm as showed in Table IV) of guard band after 40 km of SSMF and 16-QAM subcarrier mapping.

mappings, respectively. However, if we compare the results depicted in Fig. 6 (DDO-CE-OFDM system) with the results showed in Table IV and Fig. 8 of Ref. [8] (DDO-OFDM system), we can conclude that, for the same guard bands (≈ 32 and 34%), power gains around 6.0 and 5.0 dB are achieved for 4-QAM and 16-QAM, respectively, if CE-OFDM signals are employed in the 40 km of SSMF link. Fig. 6.(a) also show that, with 4-QAM subcarrier mapping, an EVM -15 dB (bit error-free reception) was obtained with a fiber launch power around -8 dBm, whereas for the DDO-OFDM investigated in Ref. [8] this is achieved with an optical power of ≈ -2 dBm. For 16-QAM as the modulation in the subcarriers, an EVM of -20 dB

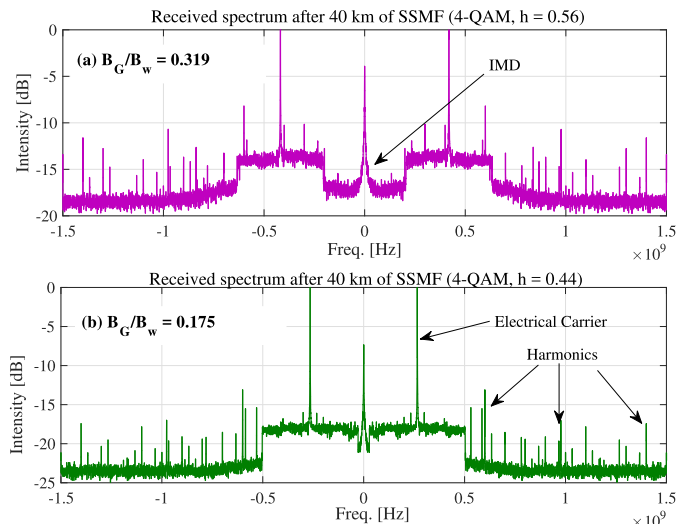


Fig. 8. Received signal spectrum for a guard band of (a) 31.9 and (b) 17.5% of signal bandwidth, for 4-QAM and 40 km of SSMF.

is reached with ≈ -5.3 and ≈ -0.6 dBm in the systems with and without constant envelope signals, considering a guard band of $\approx 34\%$.

D. Attesting the Exploitation of the Signal Dynamic Range

The constant envelope nature of its transmission signals allows a better exploitation of the DDO-CE-OFDM signal dynamic ranges, i.e., the signal amplitude A in the equation (1) can be increased in order to increase system performance.

Therefore, a performance analysis in terms of OMI is extremely important in the optimized systems. Unlike the above described results, obtained with the optimized values of OMI, Fig. 7 shows the EVM versus OMI for 4 and 16-QAM mappings, considering 17.5, 31.9 and 63.4% of guard band.

Fig. 7.(a) shows that, for 4-QAM subcarrier mapping, the DDO-CE-OFDM system should decrease the OMI from 0.34 to 0.14 to halve B_G/B_w , maintaining the performance. Fig. 7.(b) shows that, to halve the guard band at 16-QAM mapping, a reduction around 0.23 should be arranged to keep the performance ($\text{BER} \approx 1.6 \times 10^{-3}$ and $\text{EVM} \approx -15$ dB). It should be stressed that the scatterplots shown inset Fig. 7 were measured for $\text{OMI} = 0.21$ and $B_G/B_w = 0.175$ and 0.319 for 4 and 16-QAM, respectively. The fiber injection powers employed in those constellation measurements are the quantities required to obtain the EVM values that corresponds to a $\text{BER} = 1.0 \times 10^{-3}$.

The measured spectrum shown in Figs. 8.(a) and (b) confirm the SE provided by proposed multi-objective optimization procedure in DDO-CE-OFDM systems. The harmonics shown in both measurements can be mitigated or removed by phase-continuous CE-OFDM signals or by electrical frequency modulation as suggested in [5] and [16], respectively.

VI. CONCLUSION

The spectral efficiency of direct-detection optical OFDM systems based on constant-envelope signals was increased by a Multi-objective optimization procedure. A Genetic algorithm

was implemented to minimize the recommended optical guard-band between the CE-OFDM signals and the optical carrier, optimizing the fiber input power required to achieve a BER $\leq 10^{-3}$.

Simulation results show that, after propagation over 40 km of uncompensated SSMF, guard-band reduction around 55% and 40% was achieved for 4-QAM and 16-QAM subcarrier mapping, with -10.5 and -7 dBm fiber input power, respectively. With a proper optimization of both electrical phase modulation and optical modulation indices, those reductions can reach 81% and 66% for 4-QAM and 16-QAM mapping, respectively, with power penalties of approximately 6 and 2 dB demanded by the inherent spectral broadening of CE-OFDM signals.

An experimental proof-of-concept was conducted to validate the optimization procedure, under the transmission of 2 Gbps (4-QAM) and 4 Gbps (16-QAM) optimized DDO-CE-OFDM systems over 40 km of uncompensated SSMF. Experimental results prove that the spectral efficiency of optical OFDM direct-detection systems with constant-envelope signals in short-range links can be increased, regarding the trade-off between guard-band and fiber injection power.

REFERENCES

- [1] J. P. J. Z. M. G. S. Thompson and A. Ahmed, "Constant envelope OFDM," *IEEE Trans. Commun.*, vol. 56, no. 8, pp. 1300–1312, Aug. 2008.
- [2] J. A. L. Silva, T. M. Alves, A. Cartaxo, and M. E. Segatto, "Experimental demonstration of a direct-detection constant envelope OFDM system," in *Advanced Photonics & Renewable Energy, OSA Technical Digest (CD)* (Optical Society of America), Paper SPTb2, 2010.
- [3] J. Silva, A. Cartaxo, and M. Segatto, "A PAPR reduction technique based on a constant envelope OFDM approach for fiber nonlinearity mitigation in optical direct-detection systems," *IEEE/OSA J. Opt. Commun. Netw.*, vol. 4, no. 4, pp. 296–303, Apr. 2012.
- [4] R. B. Nunes, H. R. de O. Rocha, M. E. Segatto, and J. A. Silva, "Experimental validation of a constant-envelope OFDM system for optical direct-detection," *Opt. Fiber Technol.*, vol. 20, no. 3, pp. 303–307, 2014.
- [5] C. Chung, "Spectral precoding for constant-envelope OFDM," *IEEE Trans. Commun.*, vol. 58, no. 2, pp. 555–567, Feb. 2010.
- [6] M. S. Moreolo, R. Munoz, and G. Junyent, "Novel power efficient optical OFDM based on Hartley transform for intensity-modulated direct-detection systems," *J. Lightw. Technol.*, vol. 28, no. 5, pp. 798–805, Mar. 2010.
- [7] J. Ma and H. Liang, "A novel optical transmission link with DHT-based constant envelope optical OFDM signal," *Opt. Commun.*, vol. 300, pp. 33–37, Jul. 2013.
- [8] E. da V. Pereira, H. R. de O. Rocha, R. B. Nunes, M. E. V. Segatto, and J. A. L. Silva, "Impact of optical power in the guard-band reduction of an optimized DDO-OFDM system," *J. Lightw. Technol.*, vol. 33, no. 23, pp. 4717–4725, Dec. 2015.
- [9] L. Deng, X. Pang, I. T. Monroy, M. Tang, P. Shum, and D. Liu, "Experimental demonstration of nonlinearity and phase noise tolerant 16-QAM OFDM W-band (75110 GHz) signal over fiber system," *J. Lightw. Technol.*, vol. 32, no. 8, pp. 1442–1448, Apr. 2014.
- [10] S.-H. Fan, J. Yu, and G.-K. Chang, "Optical OFDM scheme using uniform power transmission to mitigate peak-to-average power effect over 1040 km single-mode fiber," *J. Opt. Commun. Netw.*, vol. 2, no. 9, pp. 711–715, Sep. 2010.
- [11] A. Abdalla, M. Lima, and A. Teixeira, "Reduced bandwidth transmitter and simple detection scheme for improved constant envelope OFDM," *Electron. Lett.*, vol. 47, no. 6, pp. 391–392, Mar. 2011.
- [12] B. J. C. Schmidt, A. J. Lowery, and J. Armstrong, "Experimental demonstrations of electronic dispersion compensation for long-haul transmission using direct-detection optical OFDM," *J. Lightw. Technol.*, vol. 26, no. 1, pp. 196–203, Jan. 2008.
- [13] K. Deb, *Multi-Objective Optimization Using Evolutionary Algorithms*, vol. 16. Hoboken, NJ, USA: Wiley, 2001.
- [14] J. Drezo, A. Petrowski, P. Siarry, and E. Taillard, *Metaheuristics for Hard Optimization: Methods and Case Studies*. New York, NY, USA: Springer Science & Business Media, 2006.
- [15] R. Schmogrow *et al.*, "Error vector magnitude as a performance measure for advanced modulation formats," *IEEE Photon. Technol. Lett.*, vol. 24, no. 1, pp. 61–63, Jan. 2012.
- [16] V. K. Singh and U. Dalal, "Abatement of PAPR for ACO-OFDM deployed in VLC systems by frequency modulation of the baseband signal forming a constant envelope," *Opt. Commun.*, vol. 393, pp. 258–266, Jun. 2017.

Helder Roberto de O. Rocha was born in Santo Antão, Cabo Verde. He received his B.S. degree in electrical engineering in 2002 and his M.S. and D.S. degrees in computing science in 2005 and 2010 from the Federal University of Fluminense (UFES), Rio de Janeiro, Brazil. In 2013, he joined the Department of Computing and Electronic of UFES and in 2018 the Department of Electrical Engineering of UFES. His research interest includes optimization in power and telecommunication systems.

Vinicius O. C. Dias was born in Vila Velha, Brazil. He received the B.Sc. in electrical engineering and the M.Sc. in mathematics from the Federal University of Espírito Santo (UFES), Brazil. During his bachelor's degree, he developed researches related to optical communications in the UFES Telecommunications Laboratory (LabTel). He is currently a Ph.D. student at Eindhoven University of Technology (TU/e), Eindhoven, The Netherlands.

Esequiel da Veiga Pereira was born in Santiago, Cabo Verde. He received the B.S. and M.S. degrees in electrical and computers engineering in 2011 from the Faculty of Engineering of the University of Porto, Porto, Portugal and the D.S. degree in electrical engineering from UFES in 2017. In 2018, he joined the Department of Computing and Electronic of UFES. His research interests include optical fiber communication, orthogonal frequency-division multiplexing (OFDM) direct detection, and coherent-detection optical systems.

Reginaldo Barbosa Nunes received the D.S. degree in electrical engineering from the Federal University of Espírito Santo (UFES), Vitória, Brazil, in 2016. In 1997, he joined the Department of Electrical Engineering of UFES. His research interests include OFDM direct-detection and passive optical networks.

Marcelo E. V. Segatto received the B.S. degree in electrical engineering from UFES, Vitória, Brazil, the M.Sc. degree in telecommunications from the Universidade Estadual de Campinas, Brazil, and the Ph.D. degree in physics from the Imperial College London, U.K., in 1991, 1994, and 2001, respectively. In 1994, he joined the Department of Electrical Engineering of UFES. Currently, his main research interests include fiber-optic communication devices, sensors, systems, and networks. He is a member of OSA.

Jair A. L. Silva was born in So Vicente, Cabo Verde. He received the B.S., M.S., and Ph.D. degrees in electrical engineering from UFES, Vitória, Brazil, in 2003, 2006, and 2011, respectively. In 2012, he joined the Department of Electrical Engineering of UFES. His research interests include optical fiber communication, OFDM, and PON.